Proceedings of the 5th International Conference on Nonlinear Dynamics
ND-KhPI2016
September 27-30, 2016, Kharkov, Ukraine

Nonlinear Dynamic Analysis of Elastic Rotor with Disk on Cantilevered End Supported on Angular Contact Ball Bearings

Sergey V. Filipkovskiy[1*]

Abstract.
The mathematical model of rotor nonlinear oscillations on angular contact ball-bearings has been developed The disk is fixed on the console end of the shaft. The shaft deflection and the elastic deformation of the bearings have the same order. The free oscillations have been analyzed by nonlinear normal modes. The modes and backbone curves of rotor nonlinear oscillations have been calculated Oscillations are excited by the simultaneous action of the rotor unbalance and vibration of supports. The frequency response, orbits and Poincaré maps have been constructed on the mode when rotating speed of the rotor is in the frequency range of supports vibration. The analysis of nonlinear dynamics of the rotor has shown that besides the main resonance at low frequencies there are superresonant oscillations. The unstable modes saddle-node bifurcations leading to beats are observed

Keywords: rotor, angular contact ball-bearing, oscillations, nonlinear normal modes, backbone curve, frequency response, bifurcation.

[1]Kharkov National Automobile and Highway University, Kharkov, Ukraine
*** Corresponding author:** svfil@inbox.ru

Introduction

The analysis of nonlinear dynamics of machines allows to predict destructive oscillations in conditions which are safe from the point of view of the linear model of the system, and to reduce their material consumption and terms of design due to more precise calculations. Practically all vehicles contain rotors supported by nonlinear bearings. Nonlinearity of ball-bearings is caused by clearances between balls and races, and nonlinear dependence of contact forces on deformations. The nonlinear analysis of rotors on ball-bearings with clearances is given in articles [1,2,3]. Closing clearances in ball-bearings causes shock loads and excessive vibrations. In order to reduce them angular-contract bearings with axial preload are used. Nonlinear dynamics of such rotors is investigated in papers [4,5]. The influence of the contact angle of the ball bearing and axial preloads on nonlinear dynamics of the rotor is analyzed in paper [6].

In the majority of works the oscillations of rotors in which one disk is positioned in the middle between supports are considered, these oscillations being caused by unbalance or bearings defects. In such models the deformed shaft center line is approximated, as a rule, by harmonic functions. In many machines the rotor on axial preloaded angular contact ball-bearings has a disk on the console end, and the bearings are mounted on the vibrating basis. The tasks of creation of a mathematical model and development of a technique to research oscillations of the rotor on axial preloaded angular contact ball-bearings, as well as the analysis of dynamics of the rotor when the frequency of its rotation is in the range of frequencies of the basis vibration are set in this paper.

1. Equations of Rotor Oscillations

It is difficult to apply harmonic functions for approximation of the axis of the deformed shaft in the rotor of such structure therefore we use the finite-element method. The design model of the rotor is presented in Figure 1. The finite elements approximate the parts of the shaft of constant section. Disks and supports are placed in nodes. Numbers of nodal sections are denoted in Figure 1 by numbers 1 – 5. We consider forces and the moments of forces of the disk inertia, as well as contact forces arising in bearings, as boundary conditions in the corresponding nodes.

Free oscillations of a shaft of constant section are described by the following equations [7]:

$$EI\frac{\partial^4 u_x}{\partial \zeta^4} + \rho F\frac{\partial^2 u_x}{\partial t^2} = 0 ,$$

$$EI\frac{\partial^4 u_y}{\partial \zeta^4} + \rho F\frac{\partial^2 u_y}{\partial t^2} = 0 . \tag{1}$$

where I and F – are the second moment of area and the cross-sectional area of the shaft, respectively, E and ρ – are the Young modulus and the mass density of the shaft, respectively.

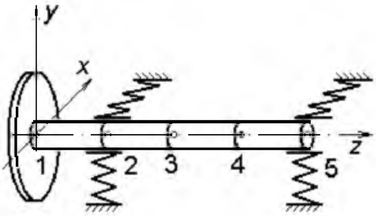

Figure 1. Finite elements of the rotor and the nodes on the ends of elements (1 – 5)

Coordinate axes are directed, as shown in Figure 1. The generalized coordinates which are the components of the vector of nodal displacements of a node i are placed in the following order: $u_{i,1} = u_{i,x}$, $u_{i,2} = \theta_{i,y}$, $u_{i,3} = u_{i,y}$, $u_{i,4} = \theta_{i,x}$, $u_{i,5} = u_{i,z}$. Interpolation polynoms of the finite element are the functions of a bending line of the beam with single movements of nodal sections.

The equations of oscillations of the shaft are received by Galerkin's method at simultaneous approximation of the equations and boundary conditions [8]

$$\int_{O} W_e R_O dO + \int_{\Gamma} \overline{W}_e R_\Gamma d\Gamma = 0 , \tag{2}$$

where R_O is a residual of the solution of the equation, R_Γ is a residual in boundary conditions, W_e and $\overline{W}_e$ are the weight functions in the area and on border, respectively, e is a number of finite element. As weight functions in this method we take interpolation polynoms $W_e \equiv N_e$.

If expressions (1) are substituted into the first integral (2) we receive the following integrals longwise of the element

$$\int_0^l [N_e]^{\mathrm{T}} \left(EI\frac{\partial^4 u_x}{\partial \zeta^4} + \rho F\frac{\partial^2 u_x}{\partial t^2} \right) d\zeta ,$$

$$\int_0^l [N_e]^{\mathrm{T}} \left(EI\frac{\partial^4 u_y}{\partial \zeta^4} + \rho F\frac{\partial^2 u_y}{\partial t^2} \right) d\zeta , \tag{3}$$

where $[N_e]^{\mathrm{T}}$ is a vector of interpolation polynoms.

Carrying out integration by parts in (3) for terms, which contain derivatives by coordinate ζ, we receive

$$\int_0^l [N_e]^{\mathrm{T}} \left(EI\frac{\partial^4 u_x}{\partial \zeta^4} \right) d\zeta = [K_e][u_{i,1} \quad u_{i,2} \quad u_{i+1,1} \quad u_{i+1,2}]^{\mathrm{T}} ,$$

$$\int_0^l [N_e]^{\mathrm{T}} \left(EI\frac{\partial^4 u_y}{\partial \zeta^4} \right) d\zeta = [K_e][u_{i,3} \quad u_{i,4} \quad u_{i+1,3} \quad u_{i+1,4}]^{\mathrm{T}} , \tag{4}$$

where $[K_e]$ is a stiffness matrix of the finite element. Carrying out integration in (3) for terms with derivatives on time we receive

$$\int_0^l [N_e]^{\mathrm{T}} \left(\rho F \frac{\partial^2 u_x}{\partial t^2} \right) d\zeta = [M_e] [\ddot{u}_{i,1} \quad \ddot{u}_{i,2} \quad \ddot{u}_{i+1,1} \quad \ddot{u}_{i+1,2}]^{\mathrm{T}},$$

$$\int_0^l [N_e]^{\mathrm{T}} \left(\rho F \frac{\partial^2 u_y}{\partial t^2} \right) d\zeta = [M_e] [\ddot{u}_{i,3} \quad \ddot{u}_{i,4} \quad \ddot{u}_{i+1,3} \quad \ddot{u}_{i+1,4}]^{\mathrm{T}}; \qquad (5)$$

where $[M_e]$ is a matrix of mass of the finite element. The components of lines and columns of matrixes corresponding to movement u_z will be zero because the shaft is not deformed along the rotation axis, except for a diagonal component of the matrix of masses which is equal to the mass of finite element.

The first boundary condition on the end of the shaft with the disk is equality of the bending moment and the moment of forces of the disk inertia

$$\left[EI \frac{\partial^2 u_x}{\partial \zeta^2} + I_1 \frac{\partial^3 u_x}{\partial \zeta \partial t^2} + I_0 \Omega \frac{\partial^2 u_y}{\partial \zeta \partial t} \right]_{\zeta=0} = 0,$$

$$\left[EI \frac{\partial^2 u_y}{\partial \zeta^2} + I_1 \frac{\partial^3 u_y}{\partial \zeta \partial t^2} - I_0 \Omega \frac{\partial^2 u_x}{\partial \zeta \partial t} \right]_{\zeta=0} = 0, \qquad (6)$$

where I_1 and I_0 are the diametrical and polar moments of the disk inertia, respectively, Ω is an angular speed of the rotor. If expressions (6) and $\zeta = 0$ are substituted into the second integral (2) we receive an additive to the matrix of masses $[M_{I1}]$ and a gyroscopic matrix $[G_1]$ for degrees of freedom of the corresponding node

$$[N_e]^{\mathrm{T}} I_1 \frac{\partial^3 u_x}{\partial \zeta \partial t^2}\bigg|_{\zeta=0} + [N_e]^{\mathrm{T}} I_1 \frac{\partial^3 u_y}{\partial \zeta \partial t^2}\bigg|_{\zeta=0} = [M_{I1}] [\ddot{u}_{1,1} \quad \ddot{u}_{1,2} \quad \ddot{u}_{1,3} \quad \ddot{u}_{1,4}]^{\mathrm{T}}, \qquad (7)$$

$$[N_e]^{\mathrm{T}} I_0 \Omega \frac{\partial^2 u_y}{\partial \zeta \partial t}\bigg|_{\zeta=0} + [N_e]^{\mathrm{T}} I_0 \Omega \frac{\partial^2 u_x}{\partial \zeta \partial t}\bigg|_{\zeta=0} = [G_1] [\dot{u}_{1,1} \quad \dot{u}_{1,2} \quad \dot{u}_{1,3} \quad \dot{u}_{1,4}]^{\mathrm{T}}. \qquad (8)$$

The second boundary condition on the end of the shaft with the disk is equality of lateral force and force of the disk inertia

$$\left[EI \frac{\partial^3 u_x}{\partial \zeta^3} + m_0 \frac{\partial^2 u_x}{\partial t^2} \right]_{\zeta=0} = 0,$$

$$\left[EI \frac{\partial^3 u_y}{\partial \zeta^3} + m_0 \frac{\partial^2 u_y}{\partial t^2} \right]_{\zeta=0} = 0, \qquad (9)$$

where m_0 is the mass of the disk. If expression (9) and $\zeta = 0$ are substituted into the second integral (2) we receive an additive to the matrix of masses $[M_{m1}]$

$$[N_e]^{\mathrm{T}} m_0 \frac{\partial^2 u_x}{\partial t^2}\bigg|_{\zeta=0} + [N_e]^{\mathrm{T}} m_0 \frac{\partial^3 u_y}{\partial t^2}\bigg|_{\zeta=0} = [M_{m1}] [\ddot{u}_{1,1} \quad \ddot{u}_{1,2} \quad \ddot{u}_{1,3} \quad \ddot{u}_{1,4}]^{\mathrm{T}}. \qquad (10)$$

If the disk is fixed on a shaft with eccentricity of a, then equations (9) will change in such a way

$$\left[EI\frac{\partial^3 u_x}{\partial\zeta^3}+m_0\frac{\partial^2 u_x}{\partial t^2}\right]_{\zeta=0}-m_0 a\Omega^2\cos\Omega t=0,$$

$$\left[EI\frac{\partial^3 u_y}{\partial\zeta^3}+m_0\frac{\partial^2 u_y}{\partial t^2}\right]_{\zeta=0}-m_0 a\Omega^2\sin\Omega t=0. \tag{11}$$

If expression (11) and $\zeta=0$ are substituted into the second integral (2) besides matrix $[M_{m1}]$ we receive a vector of the right-hand part of the equations of oscillations $\{H_D(\Omega,t)\}$ which is caused by the disk unbalance

$$\{H_D(\Omega,t)\}=m_0 a\Omega^2[\cos\Omega t \quad 0 \quad \sin\Omega t \quad 0]^{\mathrm{T}}. \tag{12}$$

For the node fixed in the bearing, the boundary conditions by axes x, y look like that:

$$-\left(EI\frac{\partial^3 u_x}{\partial\zeta^3}\right)_i+\left(EI\frac{\partial^3 u_x}{\partial\zeta^3}\right)_{i+1}-P_x(u_x,u_y,u_z)=0,$$

$$-\left(EI\frac{\partial^3 u_y}{\partial\zeta^3}\right)_i+\left(EI\frac{\partial^3 u_y}{\partial\zeta^3}\right)_{i+1}-P_y(u_x,u_y,u_z)=0, \tag{13}$$

where $P_{x,i}$ and $P_{y,i}$ are the functions of bearing restoring forces which have been received in paper [9]. If expressions (13) and $\zeta=0$, in case of the left node of an element, or $\zeta = l$, in case of the right node of an element, are substituted into the second integral (2) we receive a vector function of the bearing restoring forces

$$[N_e]_i^{\mathrm{T}}P_{x,i}(u_x,u_y,u_z)\Big|_{\zeta=l}+[N_e]_i^{\mathrm{T}}P_{y,i}(u_x,u_y,u_z)\Big|_{\zeta=l}=[P_{x,i}(u_{i,1},u_{i,3},u_z) \quad 0 \quad P_{y,i}(u_{i,1},u_{i,3},u_z) \quad 0]^{\mathrm{T}}=\{K_\Pi(U)\}. \tag{14}$$

If the rotor is mounted on the vibrating base, the vector of kinematic excitation of oscillations is added on the right side of equation [10]

$$\{H_\Pi(\omega,t)\}=-[M]\{A_\Pi(\omega,t)\}, \tag{15}$$

where $[M]$ is the matrix of masses, $\{A_\Pi(\omega,t)\}$ is the vector of supports vibration accelerations, ω is the angular frequency of supports vibration. Damping forces are concentrated in bearings, therefore the vector of damping forces has the same structure as the vector $\{K_\Pi(U)\}$. In this paper we accept model of viscous damping, then the coefficients of damping matrix $[C]$ will be placed on the diagonal in the lines which are filled in the vector $\{K_\Pi(U)\}$. Assembling the matrixes received by formulas (4), (5), (7), (8), (10) and vectors (12), (14), (15) we receive the equation of oscillations.

$$[M]\{\ddot U\}+[G]\{\dot U\}+[C]\{\dot U\}+[K]\{U\}+\{K_\Pi(U)\}=\{H_D(\Omega,t)\}+\{H_\Pi(\omega,t)\}. \tag{16}$$

2. Analysis of the Rotor Free Oscillations

The equation of free oscillations without damping has a form

$$[M]\{\ddot U\}+[G]\{\dot U\}+[K]\{U\}+\{K_\Pi(U)\}=0. \tag{17}$$

For the analysis of free oscillations we use the method of nonlinear normal modes which allows to bring the analysis of the system with the finite numbers of degrees of freedom to the analysis of the oscillator with a single degree of freedom [9,11].

Having multiplied (17) by $[M]^{-1}$ and having denoted the vector of generalized velocities $\{V\}=\{\dot{U}\}$ we receive the system of the first order equations

$$\{\dot{V}\}+[G']\{V\}+[K']\{U\}+\{K'_{\Pi}(\mathrm{U})\}=0, \tag{18}$$

where $[M]^{-1}[G]=[G']$, $[M]^{-1}[K]=[K']$, $[M]^{-1}\{K_{\Pi}(U)\}=\{K'_{\Pi}(U)\}$.

We present all phase coordinates as the functions of one pair of phase coordinates which can be chosen arbitrary [11]

$$\begin{Bmatrix} U \\ V \end{Bmatrix}=\begin{Bmatrix} P(p,q) \\ Q(p,q) \end{Bmatrix}, \tag{19}$$

where p is displacement and $q=\dot{p}$ is velocity. Having performed transformations we receive one differential equation of the movement by the chosen vibration mode:

$$\ddot{p}+B_1\dot{p}+B_2p+B_3p^2+B_4p\dot{p}+B_5\dot{p}^2+B_6p^3+B_7p^2\dot{p}+B_8p\dot{p}^2+B_9\dot{p}^3=0\,. \tag{20}$$

The equation (20) is solved by harmonious balance method.

3. Analysis of the Rotor Forced Oscillations

Multiplying (16) by $[M]^{-1}$ we receive the following equation

$$\{\ddot{U}\}+[G']\{\dot{U}\}+[C']\{\dot{U}\}+[K']\{U\}+[K'_{\Pi}(U)]=[M]^{-1}\{H_D(\Omega,t)\}-\{A_{\Pi}(\omega,t)\}, \tag{21}$$

where $[M]^{-1}[G]=[G']$, $[M]^{-1}[K]=[K']$, $[M]^{-1}[\mathrm{C}]=[C']$, $[M]^{-1}\{K_{\Pi}(U)\}=\{K'_{\Pi}(U)\}$. For the following analysis we introduce the dimensionless variables: $\bar{x}_n=x_n/z_0$, $\bar{y}_n=y_n/z_0$, $\bar{z}=z/z_0$, $\bar{\omega}=\omega/\omega_l$, $\bar{\Omega}=\Omega/\omega_l$, $\tau=t\cdot\omega_l$, where ω_l is the basic resonance frequency of the linearized system, we also write (21) in the form of a nonlinear vector function $\{f\}$.

$$\{\ddot{U}\}=\{f(\{U\},\{\dot{U}\},\bar{\omega},\tau)\}. \tag{22}$$

We consider velocity of the rotor rotating Ω being fixed, the angular frequency of supports vibration ω changes in the prefixed range. To construct frequency response we make the analysis of the equation (22) by a predictor-corrector continuation method [12], which also determines the monodromy matrix, stability and nature of bifurcations of the periodic solution of the equation.

4. Results of the Numerical Researches

The rotor parameters are as follows: L = 0.34 m is the shaft length; l = 0.06 m is the length of the console end; d_1 = 0.025 m is the diameter of the console end of the shaft; d_2 = 0.032 m is a diameter of a shaft between supports; $E=2.1\cdot10^{11}$ Pa and $\rho=0.3$; m = 5.0 kg, I_1 = 0.1 kg·m^2, I_0 = 0.2 kg·m^2; $f_{\Omega}=\Omega/2\pi$ = 50 Hz is the rotor rotation frequency. Oscillations are excited by unbalance of the disk whose eccentricity is a = 0.008 mm and by vibration of support with the amplitudes of $A_{\Pi x}=0$, $A_{\Pi y}=2$g. Frequency of vibration is changed in the range from 20 to 2000 Hz.

The standard angular contact ball-bearing parameters are as follows: $\alpha=15°$ is the contact angle; R_2 = 27.525 mm is the radius of the outer race; R_1 = 16.000 mm is the radius of inner race;

R_K = 5.930 mm is the race radius of curvature; d_B = 11.510 mm is diameter of the balls; N_B = 7 is the number of balls; $E = 2.1 \cdot 10^{11}$ Pa; $\mu = 0.3$.

Frequencies of transverse oscillations of the linearized system are 70.54 Hz, 110.63 Hz, 196.22 Hz and 202.11 Hz. Frequency of longitudinal oscillations of the linearized system is 101.70 Hz. Backbone curves of the rotor are shown in Figure 2. The system has soft characteristics. Curves 1 and 2 correspond to oscillations in the fundamental mode. With the bigger frequency the curved shaft axle rotates in the direction of shaft rotation, and with a smaller frequency – in the opposite direction. Curves 3 and 4 correspond to similar oscillations in the second mode.

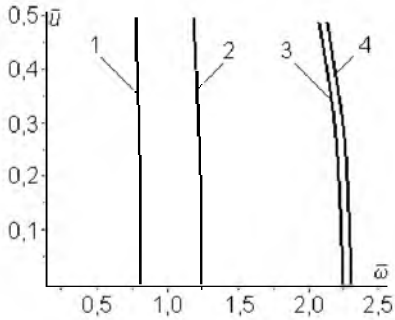

Figure 2. Backbone curves of a rotor

The fundamental mode of the shaft elastic axle at transverse oscillations when frequency is near 110 Hz is shown in Figure 3 (corresponds to curve 2 in Figure 2). With oscillations in the fundamental mode the shaft spindles are placed on the opposite sides from an axis of bearings. The mode of the shaft elastic axle when frequency is near 202 Hz is shown in Figure 4 (corresponds to curve 4 in Figure 2). In this case the shaft spindles are placed on the same side from the axis of bearings.

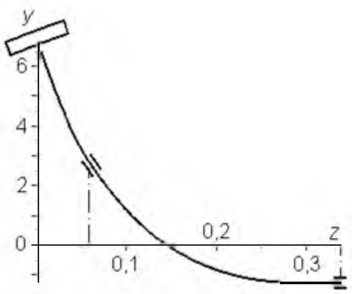

Figure 3. Fundamental mode of shaft oscillations

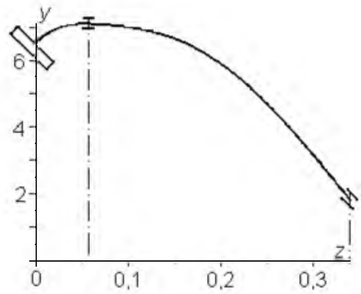

Figure 4. Second mode of shaft oscillations

5. Frequency Response Analysis

The frequency response of the rotor oscillations is shown in Figure 5. The resonance peak 1 corresponds to the oscillation mode when shaft spindles are from the opposite sides of the bearings axis and during oscillations their centers move on the elliptic orbits in the direction of shaft rotation. The resonance peaks 2 – 6 correspond to the oscillation mode when the shaft spindles are on the same side from the axis of symmetry of bearings and during oscillations their centers also move in the direction of shaft rotation. At the same time peaks 3 – 6 correspond to superresonances of order 2/1 – 5/1. Resonant oscillations in a mode when the centers of spindles move in the opposite direction are not observed.

On the left of the resonance peaks 1 and 2 the unstable oscillations are obtained which shown in Figure 5 by dashed lines. Unstable oscillations are obtained also to the right of the resonance peak 2.

6. Analysis of Stable Oscillations

Orbits of the disk and spindles centers with resonant oscillations in the fundamental mode are similar to elliptic ones, as shown in Figure 6 for the vicinity of resonance peak 2 in Figure 5. For superresonance frequencies for one period of oscillations the centers make so many loops, how many times the frequency is lower than the fundamental frequency for this mode, as shown in Figure 7 for the vicinity of resonance peak 3 in Figure 5.

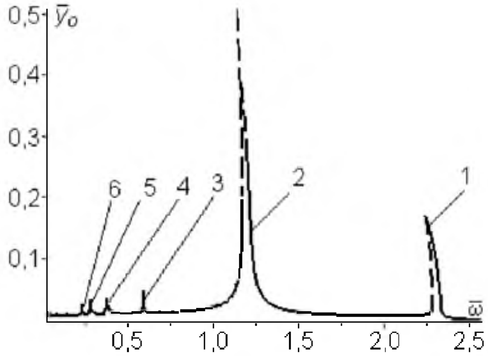

Figure 5. Frequency response

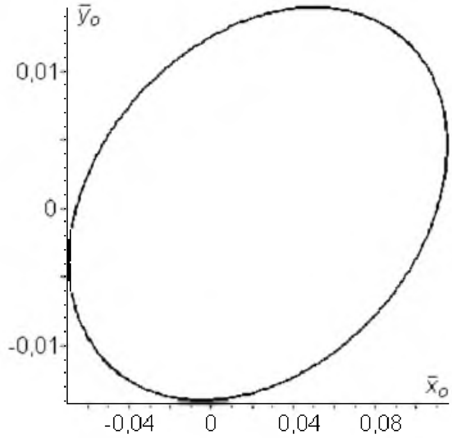

Figure 6. The orbit of disk center at $\bar{\omega} = 1{,}2466$

Superresonant oscillations have comparatively small amplitudes with more complicated orbits of the disk centre as shown in Figures 6 and 7. Apparently, such complexity of orbits in the considered example is caused by the fact that there occur superresonances of both oscillation modes. In this case the fundamental resonance frequency of the second mode is approximately twice as big as the corresponding frequency of the first mode. This results in superposition of oscillations of different modes.

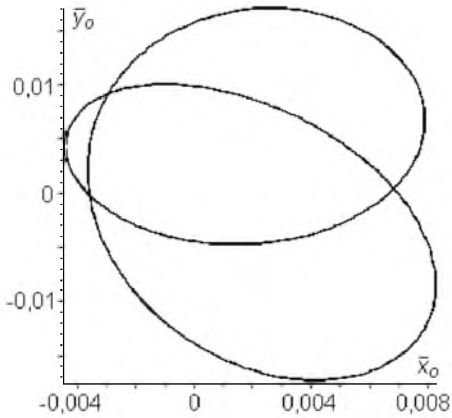

Figure 7. The orbit of disk center at $\bar{\omega} = 0{,}6236$

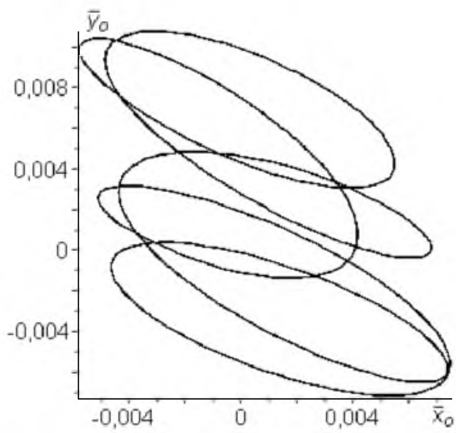

Figure 8. The orbit of disk center at $\bar{\omega} = 0{,}2493$

7. Analysis Oo Unstable Oscillations

On the left branches of the principal resonance peaks saddle-node bifurcations are obtained. Peak-to-peak displacements remain limited, but change over time rather slowly. The orbit of the disk center for ten periods on the left branch of the resonance peak 2 is shown in Figure 9. To specify the nature of the oscillatory process the Poincaré map shown in Figure 10 has been constructed. It shows that transition process leads to beats. On big peak-to-peak displacements to the right of resonance peak 2 Neimark – Sacker bifurcation which lead to similar beats are obtained.

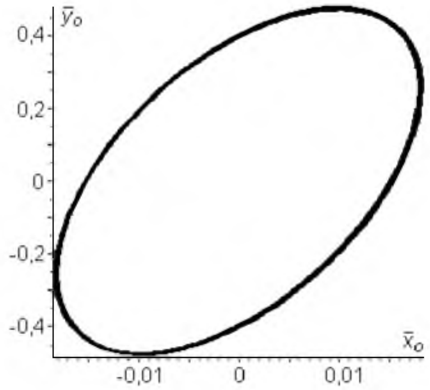

Figure 9. The orbit of disk center at $\overline{\omega} = 1{,}2142$

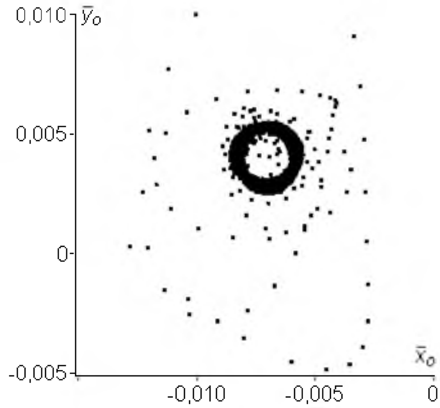

Figure 10. Poincaré map at $\overline{\omega} = 1{,}2142$

Conclusions

Oscillations of the rotor supported by the preloaded angular contact ball bearings have been investigated. The disk is fixed on the console end of the shaft. Backbone curves and non-linear normal modes by Shaw and Pierre have been obtained. The backbone curves are soft. The joint action of the unbalance and vibration of supports causes resonances of the two modes of the rotor oscillations and superresonances of order 2/1, 3/1, etc. Therefore, resonant oscillations can occur throughout the whole frequency range below the fundamental resonance frequency.

Resonances, when the shaft spindles are placed on the opposite sides of the bearings axis, have a greater displacement and lower frequency than the resonance with the shaft spindles placed on the same side of the bearing axis. To the left of the principal resonance saddle-node bifurcation is observed, and to the right is Neimark – Sacker bifurcation.

References

[1] Villa C. Sinou J.-J., Thouverez F. Stability and vibration analysis of a complex flexible rotor bearing system. *Communications in Nonlinear Science and Numerical Simulation*, Vol. 13(4), p. 804–821, 2008.

[2] Yadav H. K., Upadhyay H. Study of effect of unbalanced forces for high speed rotor. *Procedia Engineering*, Vol. 64, p. 593–602, 2013.

[3] Babu C. K., Tandon N.R., Pandey K. Nonlinear vibration analysis of an elastic rotor supported on angular contact ball bearings considering six degrees of freedom and waviness on balls and races. *Journal of Vibration and Acoustics*, Vol. 136(4), p. 044503-1-5, 2014.

[4] Panda K.C., Dutt J.K. Optimum support characteristics for rotor–shaft system with preloaded rolling element bearings. *Journal of Sound and Vibration*, Vol. 260(4), p. 731–755, 2003.

[5] Bai, C., Zhang, H., Xu, Q. Effects of axial preload of ball bearing on the nonlinear dynamic characteristics of a rotor-bearing system. *Nonlinear Dynamics*, Vol. 53, p. 173–190, 2008.

[6] Cui, L., Zheng, J. Nonlinear vibration and stability analysis of a flexible rotor supported on angular contact ball bearings. *Journal of Vibration and Control*, Vol. 20, p. 1767–1782, 2014.

[7] Dimentberg, F.M. *Flexural vibrations of rotating shaft*. London, Butterworths, 1961.

[8] Zienkiewicz, O.C., Morgan, K. *Finite elements and approximation*. John Wiley & Sons, 1983.

[9] Filipkovskii, S.V., Avramov, K.V. Nonlinear Free Vibrations of Multi-Disk Rotors on Ball Bearings. *Strength of Materials*, Vol. 45(3), p. 316–323, 2013.

[10] Timoshenko, S.P., Young, D.H., Weaver, W. *Vibration Problems in Engineering*. John Wiley & Sons, 1974.

[11] Shaw S.W., Pierre C. Normal modes of vibration for non-linear continuous systems. *Journal of Sou nd and Vibration*, Vol. 169(3), p. 319–347, 1994.

[12] Seydel R. Nonlinear computation. *International Journal of Bifurcation and Chaos*, Vol. 7, p. 2105–2126, 1997.